electronics

MDPI

Article

Double Slot Antenna for Microwave Thermal Ablation to Treat Bone Tumors: Modeling and Experimental Evaluation

Citlalli Jessica Trujillo-Romero [1,*], Lorenzo Leija-Salas [2], Arturo Vera-Hernández [2], Genaro Rico-Martínez [3] and Josefina Gutiérrez-Martínez [1]

[1] Division of Medical Engineering Research, National Institute of Rehabilitation LGII, Mexico City 14389, Mexico; jgutierrez@inr.gob.mx
[2] Electrical Engineering Department, Bioelectronics Section, CINVESTAV-IPN, Mexico City 07360, Mexico; lleija@cinvestav.mx (L.L.-S.); arvera@cinvestav.mx (A.V.-H.)
[3] Bone Tumors Service, National Institute of Rehabilitation LGII, Mexico City 14389, Mexico; grico@inr.gob.mx
* Correspondence: cjtrujillo@inr.gob.mx

Abstract: According to statistics of the American Cancer Society, the number of young people diagnosed with bone tumors is growing. Surgery and radiotherapy are the common treatments, however they have several side effects which affect the patient's life. Therefore, a cheaper and less side-effect therapy called thermal ablation has been explored. The goal of this paper is to measure the therapeutic temperatures and the viability of a double slot antenna designed to treat bone tissue by microwave ablation. The antenna (at an operating frequency of 2.45 GHz) was designed, modeled, constructed, and experimentally evaluated. The finite element method was used to predict the antenna performance by means of 2D axisymmetric models. The modeling parameters were used to build the antenna. The experimental evaluation shows that the antenna behavior is repeatable and the standing wave ratio (SWR) was around 1.5–1.8. Temperatures around 60–100 °C were achieved over the bone tissue. The antenna insertion modifies the antenna performance. An insertion lower than 3.5 cm is not recommended because the convection effects modified the tissue temperature. The thermal patterns showed a heat focus near to the slots, which makes it possible for use in the treatment of small tumors.

Keywords: thermal ablation; bone tumor; microwave ablation (MWA); finite element method (FEM); double slot antenna

Citation: Trujillo-Romero, C.J.; Leija-Salas, L.; Vera-Hernández, A.; Rico-Martínez, G.; Gutiérrez-Martínez, J. Double Slot Antenna for Microwave Thermal Ablation to Treat Bone Tumors: Modeling and Experimental Evaluation. *Electronics* **2021**, *10*, 761. https://doi.org/10.3390/electronics10070761

Academic Editor: Paolo Colantonio

Received: 22 February 2021
Accepted: 19 March 2021
Published: 24 March 2021

1. Introduction

According to the American Cancer Society, 1720 cases of bone cancer were prognosticated to be deadly for 2020 [1]. Bone tumors frequently grow up in long bones, such as femur and tibia. Unfortunately, young people around 10–40 years old are the most diagnosed. The most common treatments are surgery (amputation), radiotherapy, and chemotherapy, which develop several side effects in patients. Moreover, chemotherapy has not shown good results [2]. Since bone tumors are more common in young people, new treatments to eradicate the tumor and keep the integrity of the healthy bone must be developed. Microwave ablation (MWA) is considered a minimally invasive technique which goal is to generate coagulative necrosis of the tumor cells by increasing their temperature. In literature and in clinical practice, thermal ablation has been widely studied and biological action mechanisms have been reported so that nowadays it is well known at which temperatures cancerous tissues suffer biological damage [3–5]. Thermal damage depends on the temperature of the tissue and the exposition time. Temperatures higher than 55 °C generate ablated tissue, while temperatures around 60–100 °C produce thermal ablation, which destroys the tumor by burning malignant cells [6–8]. Finally, temperatures over 100 °C cause vaporization and carbonization, which modify the complex permittivity

of tissues and alters the MW antenna performance [9]. Thus, in order to control the therapeutic effect of the microwave ablation (MWA), the phenomena produced by different temperatures must be considered.

The heating can be achieved by the deposition of electromagnetic energy generated by some coaxial-based antennas. Coaxial-based antennas are the most common, because of their low cost, small dimensions, and easy construction. Different types of coaxial antennas, such as monopole, dipole, and helical, are described in literature [10–14] However, one of the most common are the slot antennas, where the external and the internal conductors are soldered at the tip of the antenna, while in the external conductor, a ring of metal is cut off to work as air slot [15]. Microwave antennas frequently work at 2.45 GHz and 915 MHz [3,16,17]. The medical applications for microwave heating work at frequencies in the ISM (Industrial Scientific and Medical) band. In Europe, the most frequently used frequencies are 433.05–434.79 MHz, in the USA, frequencies from 902 to 9238 MHz, and in other countries frequencies range between 2400 and 2500 MHz [18,19]. Further, 2450 MHz (2.45 GHz) is one of the most widely used in medical practice for thermal ablation. The main goal of MWA is to apply heat to the tumor without causing damage to the healthy tissue. To get an effective therapeutic outcome, input power and treatment time must be controlled. MWA has been considered as the most promising technique to treat bone tumors [20], and is highly recommended because microwaves (MW) can easily penetrate the bones [21]. Moreover, it also works better in tissues with poor electrical conductivity, like bones. Several studies have been conclusive on the success and safety of the thermal ablation (radiofrequency and microwaves) to treat bone [22–25], liver and breast tissues [20,26,27]. MWA can be applied by making a small percutaneous incision, making an entry hole through the cortical bone [28], ultrasound or computerized tomography are used to guide the small antenna inside the tissues. The open surgery approach is used just in cases where a percutaneous procedure could not be possible due to the tumor location [29].

The current ablation studies done for bone tissue had been made by using MW commercial equipment, which were designed to treat soft tissue [17,21], which points to the need for the development of antennas specifically to treat bone. Using antennas specifically designed to treat bone tissue could help to reduce input power, treatment time and power losses [30–33]. Literature shows that the use of this technique to treat bone tumors needs a better understanding [17,20,34] making it important to develop new studies based on experimentation and modeling. To improve and better understand the MWA treatments, it is necessary to implement modeling studies to analyze the tissue absorption of electromagnetic (EM) energy, and the temperature distribution generated by such energy [35]. One of the biggest challenges in modeling is to emulate tissue properties and structure. However, although more realistic tissue properties are required, the main simplification reported in literature is to consider the human tissue as a uniform, linear, isotropic and no thermal dependent media [18,36–39]. Despite this simplification, the models have provided reliable results [35,39–41]. Although several researches deal with the dependence from the temperature of dielectric and thermal properties, most of them are focused on liver and muscle tissue. It is important to remark that the temperature dependence of bone dielectric and thermal properties has not been studied yet. Nevertheless, more computational modeling and experimental studies are required to understand the effect of dielectric and thermal tissue properties, especially for bone ablation.

A double slot antenna designed to treat specifically bone tumors is proposed. The antenna was designed, modeled, constructed, and experimentally evaluated in order to measure its feasibility to be used in the treatment of bone tumors. The antenna performance was calculated using 2D axisymmetric models with COMSOL Multiphysics® (Stockholm, Sweden), which is a commercial software based on the finite element method. The models were based on the coupling of the electromagnetic wave and the bioheat equation. Temperature profiles and patterns were obtained to evaluate the behavior of the antenna. Moreover, an experimental evaluation, in healthy porcine bones, of the antenna was done.

2. Materials and Methods

2.1. Design of the Double Slot Antenna to Treat Bone Tissue

The double slot antenna was chosen to focus the MW energy over a specific region (tumor) without damaging healthy tissue. In this antenna, the slots work as a guide to the EM radiation. The antenna was designed by using the bone effective wavelength in order to achieve a localized power deposition near the slots of the antenna that is going to be inserted into the bone tissue [10,42]. To calculate the slot location over the antenna, the effective wavelength, described by Equation (1), was used [10].

$$\lambda_{eff} = \frac{c}{f\sqrt{\varepsilon_r}}, \quad (1)$$

where c is the speed of light in free space (m/s), f is the work frequency (2.45 GHz) and ε_r is the relative permittivity of cancellous bone at 2.45 GHz (18.54) [43]. Cancellous bone was chosen because bone tumors grow up specially at the extremities of long bones, which are composed mainly by this kind of bone. The antenna length was fixed to 70 mm in order to support better manageability and avoid deformation. Preliminary research has determined that the optimal antenna design should be achievable by considering slots widths between 1 and 10 mm [44]. Therefore, the length of each slot was 1 mm and they were located at $\lambda_{eff}/8$ = 3.55 mm from the antenna tip and $\lambda_{eff}/4$ = 7.10 mm from the first slot. The slot locations were chosen in order to generate a localized power deposition near to the distal tip of the antenna. Figure 1a describes the geometry and dimensions of the double slot antenna. The antenna diameters (ϕ) were taken from a standard copper 50 Ω semi-rigid cable UT-047.

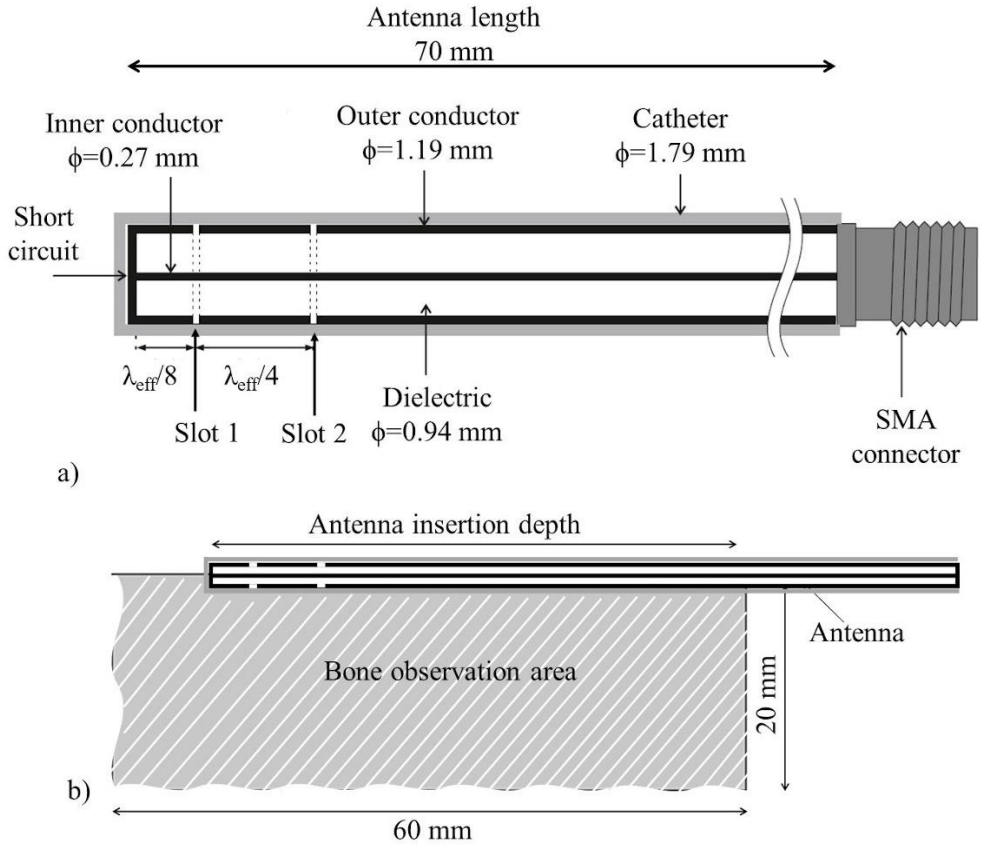

Figure 1. Geometry description of the proposed antenna, (**a**) 2D view of the proposed double slot antenna, (**b**) 2D axisymmetric model used to determine the outcome when bone tissue (observation area) is irradiated.

2.2. 2D Antenna Modeling by the Finite Element Method

The Finite Element Method (FEM) is a powerful tool to study the antenna performance. Due to its rotational symmetry, an axisymmetric antenna can be simulated in a two-dimensional domain (2D) corresponding to its angular cross section [45]. The electromagnetic wave propagating in a coaxial cable can be described by transverse electromagnetic fields (TEM). By considering time-harmonic fields, the wave propagation can be described by Equations (2)–(4) [46]:

$$E = e_r \frac{C}{r} e^{j(\omega t - kz)}, \tag{2}$$

$$H = e_\varphi \frac{C}{rR} e^{j(\omega t - kz)}, \tag{3}$$

$$P_{av} = e_z \pi \frac{C^2}{Z} \ln\left(\frac{r_{inner}}{r_{outer}}\right), \tag{4}$$

where z is the direction of propagation, and r, φ, and z are the cylindrical coordinates of the coaxial cable. P_{av} is the averaged power flow, Z is the wave impedance in the dielectric of the cable, r_{inner} and r_{outer} correspond to the radio for the outer and inner conductor, ω is the angular frequency, k is the propagation constant, which is related to the wavelength in the medium (λ), as described by Equation (5)

$$k = \frac{2\pi}{\lambda}, \tag{5}$$

The equations that govern the antenna behavior are the Maxwell's equations, described by Equations (6)–(9) [45]

$$\nabla \times E = -j\omega \overleftrightarrow{\mu} \cdot H - M_{imp}, \tag{6}$$

$$\nabla \times H = -j\omega \overleftrightarrow{\varepsilon} \cdot E - J_{imp}, \tag{7}$$

$$\nabla \cdot \left(\overleftrightarrow{\varepsilon} \cdot E\right) = -\frac{1}{j\omega} \nabla \cdot J_{imp}, \tag{8}$$

$$\nabla \cdot \left(\overleftrightarrow{\mu} \cdot H\right) = -\frac{1}{j\omega} \nabla \cdot M_{imp}, \tag{9}$$

where M_{imp} is the magnetic current density, J_{imp} is the current source that excited the antenna. This current irradiates the electromagnetic (EM) field that is modified by the antenna body. Finally, $\overleftrightarrow{\varepsilon}$ and $\overleftrightarrow{\mu}$ are the permittivity and permeability of the materials where the antenna is embedded. To correctly determine the antenna performance, it is important to define the boundary conditions. Because the antenna irradiates an EM field to the infinity, the solution space must be limited to a finite space (S_0) [45]. Therefore, the boundary must be completely transparent, i.e., the EM field could pass through the space without reflections (first-order absorbing boundary condition). This boundary condition is described by (10)

$$\hat{n} \times \nabla \times \begin{pmatrix} E \\ H \end{pmatrix} + jk_0 \hat{n} \times \hat{n} \times \begin{pmatrix} E \\ H \end{pmatrix} \approx 0 \qquad r \epsilon S_0\,, \tag{10}$$

where $\hat{n}$ is the unit vector normal to S_0, pointing toward the exterior space and k_0 is the free space wavenumber. The finite space (S_0) must be set at least on a half-wavelength away from the antenna. To model the antenna body, the boundary condition described by Equation (11) must be applied [45].

$$n \times E = 0 \qquad r \epsilon S_{PEC}, \tag{11}$$

where S_{PEC} is the perfect electrically conducting (PEC) surface of the antenna body. The antenna feed is defined as a port boundary condition; this is a first-order low-reflecting boundary condition that has an input filed $H\varphi$, described by Equation (12) [46,47]

$$n \times \sqrt{\varepsilon E} - \sqrt{\mu H_{\varphi}} = -2\sqrt{\mu H_{\varphi 0}}, \quad (12)$$

where

$$H_{\varphi 0} = \frac{\sqrt{\frac{P_{av} Z}{\pi r ln\left(\frac{r_{outer}}{r_{inner}}\right)}}}{r}, \quad (13)$$

To find the numerical solution to these equations, the finite element method must be applied. In this case, a modeling study to predict the antenna performance was done. Electromagnetic and thermal simulations were solved by the finite element method by using COMSOL Multiphysics (v4.4, COMSOL Inc., (Stockholm, Sweden)). The electromagnetic (EM) simulation was done for the antenna operating frequency of 2.45 GHz, while the thermal simulation was calculated in the time dependent domain. Due to the antenna's symmetry, and to reduce the computation time, a 2D axisymmetric model was implemented (see Figure 1b). The model consists of the micro coaxial antenna inserted in the bone tissue (6 cm × 2 cm). Several kinds of tumors are described in literature. However, although bone tumors are a real problem, the lack of information about the thermal dependence of their dielectric and thermal properties is still a problem. The lack of this information made us consider just healthy bone tissue in the models. A quantification of the thermal effect in bone, without taking into account other tissues, was analyzed. The modeled antenna is depicted in Figure 1b. The antenna was encased in a catheter, to prevent adhesion of the antenna to the burned tissue.

2.2.1. Electromagnetic Models

The EM simulation was used to calculate the specific absorption rate (*SAR*), which represents the electromagnetic energy deposited by unit of mass in the tissue (W/kg) [48]. The *SAR* was obtained by Equation (14) [10]:

$$SAR = \frac{\sigma}{2\rho}|E|^2 \quad (14)$$

where σ (S/m) is the conductivity, ρ (kg/m^3) is the bone tissue density and E is the vector of electric field strength generated by the antenna. The slots were defined as air, the antenna boundaries as perfect electric conductors and the excitation boundary as a coaxial port, fed by an antenna input power (10 W). All tissue boundaries were assigned as a scattering boundary condition, to ensure that the EM wave would pass without any reflection. Tissue dielectric properties at 2.45 GHz were used in the model implementation. It is important to mention that this is a first approach and temperature dependence of dielectric and thermal properties was not considered. Furthermore, constant property values were used in order to reduce complexity and computation resources. However, the future work might consider the effect of temperature dependence of tissue properties; moreover, the influence of the other involved tissues such as muscle and fat must be also study. Table 1 shows the dielectric and thermal properties for cancellous bone and the materials that were considered in the models. The typical mesh used in these 2D models consists of 3000 elements, approximately with a minimum element size of 0.024 mm. Figure 1b describes the 2D geometries used in the analysis of the MWA in bone tissue.

Table 1. Dielectric and thermal properties for analyzed electro-thermal model [43,49,50].

Property	Value
Electrical conductivity of bone	0.805 S/m
Thermal conductivity of bone	0.31 W/m·K
Density of bone	1908 kg/m^3
Blood density	1060 kg/m^3
Heat capacity of blood	3700 J/kg·K
Heat capacity of bone	1313 J/kg·K
ε_r of dielectric	2.03
ε_r of catheter	2.60
ε_r of bone	18.548

2.2.2. Thermal Models

The specific absorption rate (*SAR*) calculated by the previously generated electromagnetic model was used as a source for the thermal simulations [48]. The method most commonly used to model heat transfer in tissue is by the bioheat equation described by Pennes in 1948 [51]. This equation models the impact of perfusion as an isotropic heat sink. Equation (15) describes the bioheat equation.

$$\rho C \frac{\partial T}{\partial t} = \nabla \cdot (k \nabla T) + \rho Q + \rho SAR - \rho_b C_b \rho W_b (T - T_b) \quad (15)$$

where C (J/kg/K) represents the heat capacity, ρ (kg/m^3) density, k (W/m/K) thermal conductivity, ρ_b (kg/m^3) blood density, C_b (J/kg/K) heat capacity of blood, W_b (kg/m^3/s) blood perfusion, T_b (K) blood temperature, Q (W/kg) rate of heat generated by metabolism and SAR (W/kg) the specific absorption rate. In this model, the heat generated by the metabolism was neglected. The perfusion was considered with a value equal to zero (as in the experimental evaluation). The antenna input power (10 W) was applied for 10 min. The thermal simulations were made taking into account just the bone domain.

2.3. Antenna Construction

The double slot antenna was constructed by following the parameters obtained from the design: i.e., the antenna length, slot length, slot location, etc. were used to construct the antenna. A standard copper 50 Ω semi-rigid cable UT-047 (1.19 mm) and SMA 50 Ω connectors were used. The 1 mm slots of the antenna were made by using a chemical process with ferric chloride [52]. Figure 2 shows the constructed double slot antenna. The antenna has a SMA connector to be connected to the MW system.

Figure 2. Double slot antenna.

2.4. Experimental Evaluation

Microwave (MW) System, Temperature Measurements and Standing Wave Ratio (SWR)

To generate the microwaves, the ISYS245 microwave generator (Emblation Microwave, (Alloa, Scotland, UK)) was used. This is a microwave generator and amplifier system that works at 2.45 GHz. This equipment has the capability of measuring the reflected power. Additionally, four non-EM interfering temperature sensors (M3300, Luxtron, (Santa Clara, CA, USA)) were used to measure the temperature increase. In order to evaluate the impedance-matching between the proposed antenna and the transmission line [53], the

standing wave ratio (SWR) was measured. The ideal SWR value is 1, i.e., all the input power is transmitted to the tissue. Therefore, a high SWR value (greater than 1) indicates power losses. The SWR was measured at the beginning of the experiments when the antenna was inserted over the porcine bone. An Agilent Technologies network analyzer (E5071B) was used to obtain the SWR of the whole system, specifically at 2.45 GHz.

2.5. Thermal Ablation Experiments

Several researchers have shown that porcine tissue properties are not significantly different to those from the human tissues [50,54]. Therefore, several porcine femur bones (from a common butcher shop) were used to analyze and evaluate the therapeutic temperatures generated by the antenna. In each experiment, the antenna was fed with an input power of 10 W and the bone was exposed for 10 min. Some previous experimentation was done in order to choose the adequate input power and treatment time, i.e., the ideal parameters needed to reach temperatures around 55 °C–100 °C and generate ablation over the bone. 600 s (10 min) of treatment were chosen in order to analyze the behavior of the temperature and to evaluate the effect over the covered area. Temperature profiles, in specific points, were recorded during all the experimentation. The initial bone temperatures were kept around 34 °C–37 °C, in all the cases, by using a water bath. The experimental set up is depicted in Figure 3a. To evaluate the antenna outcome, two different experiments were carried out.

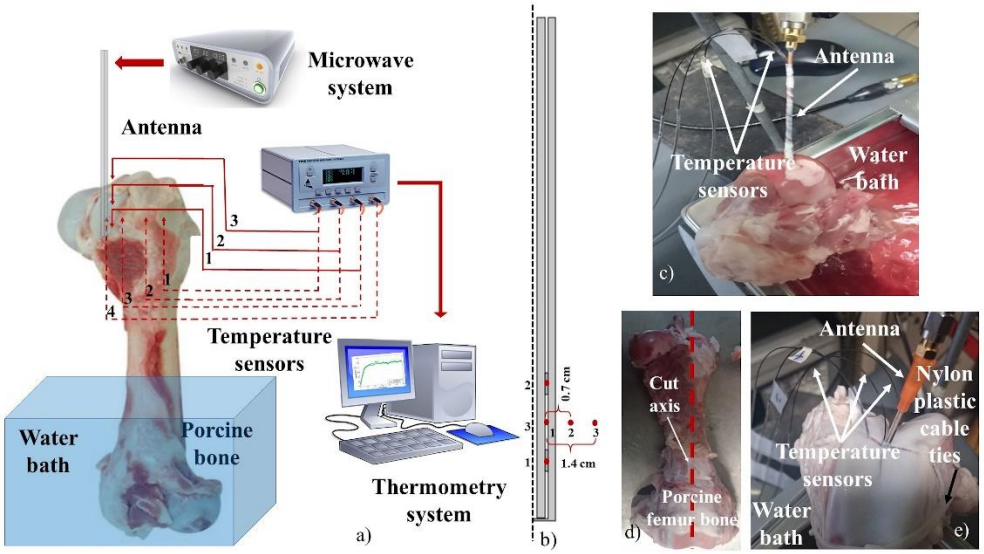

Figure 3. Experimental set up used to make the antenna evaluation in a porcine bone (femur). (**a**) equipment used in the experimental evaluation; (**b**) location of temperature sensors used in the antenna evaluation; (**c**) set up used for the antenna insertion evaluation; (**d**) incision of the porcine bone tissue; (**e**) set up for the thermal distribution evaluation.

2.5.1. Antenna Insertion

It is important to evaluate the possible effects of the antenna insertion over the temperature profiles achieved in bone tissue. According to the size of the pig bone used in each experiment, different levels of antenna insertion were evaluated. The antenna requires a deeper insertion into the bone, in order to cover both slots. It is important to remark that the thermal ablation experiments were done by using different porcine bones. However, the behavior of the antenna was evaluated under the same conditions. To insert the antenna to the femur condyle, a hole of 1.8 mm of diameter was made with a hand drill. The temperature sensors were fixed to the antenna body with Teflon tape to avoid possible movements. In order to measure the temperature over the tissue, and not the temperature of the antenna, first the antenna was covered with an initial layer of Teflon tape, then the sensors were located in the specific points and fixed with another layer of tape; the tips

of the sensors were not covered to ensure that they were in contact with the bone tissue. To evaluate the repeatability of the antenna behavior, three repetitions of each experiment were performed. The experiments were done with 3.5 cm and 5 cm of antenna insertion. The first and the second temperature sensors were located right next to the first and the second slots, while the last one was at the middle point between both slots. A complete description of sensor location is described in Figure 3b. Figure 3c shows an example of the experiment carried out to analyze the effect of antenna insertion.

2.5.2. Thermal Distributions

The thermal distribution generated by the antenna was obtained. Through the experiment, the temperature increase was measured by four temperature sensors. In order to locate the antenna and sensors, each pig femur bone was cut off by following the long middle axis line (see Figure 3d). The antenna and sensors were fixed between both pieces, which were tied with a nylon plastic cable to reshape the porcine bone. After 10 min, the MWA equipment was turned off, and the antenna was pulled out of the bone. The nylon plastic cable was cut, and the two pieces of bone were prepared for a thermal photography. A thermographic camera TI32 was used (Fluke corporation, (Everett, WA, USA)) to get the thermal distributions in bone. These images were done in order to visualize the thermal distribution generated by the antenna. However, some loses due to thermal conduction are presented from the end of the experiment to the moment in which the pictures were taken: i.e., although the generated pattern corresponds to the heated region, the temperature values (of each thermal image) could not correspond to the real ones. For this reason, four temperature sensors were used to record it. Previous results showed that antenna insertion plays an important role in the antenna performance. Therefore, in order to avoid any deformation of the thermal distribution generated by the antenna, insertions of 3.5 cm and 5 cm were analyzed. The first and the second temperature sensors were located next to the first and the second slots, while the other two sensors were located at the middle point between both slots, but at 0.7 cm and 1.4 cm. A description of sensor location is presented in Figure 3b. Figure 3e shows a picture of an experiment carried out for this study.

3. Results

3.1. 2D Antenna Modeling and Experimental Evaluation

Since the experimentation was done in ex-vivo tissue, the simulations were performed in the absence of perfusion (Wb = 0 mL/min/kg). The 2D FEM models were generated, evaluated, and compared with the experimental results. To analyze the convergence of the FEM model and to select the correct mesh size, different mesh sizes were tested, and the outcome results were analyzed. A mesh with 1209 elements generated a maximum temperature of 106 °C and a deformed thermal pattern. From 2119 to 265,048 mesh elements, the maximum temperature was 105 °C and the thermal pattern tends to be uniform and repeatable. To reduce the solution time, a refined mesh of 2795 elements was chosen to solve the analyzed model. A FEM model with a mesh of 265,048 elements took 10 min to be solved. The FEM models were run in a computer with an intel core i5-3337U processor at 1.80 GHz with 8 GB of RAM memory.

Table 2 shows the highest temperatures achieved, after 30 s and 600 s during the experimentation as well as in the FEM modeling. A maximum temperature of 152.6 °C was obtained. Although after 600 s, the discrepancies between simulation and experimentation tends to be higher, if a short exposition time is analyzed (30 s), the differences are smaller (see Table 2), especially, for those located at slot 2 and between the slots. Although after 30 s, the temperatures barely reached the therapeutic thresholds for ablation, it could be possible to use a higher level of input power (>10 W) to reach temperatures higher than 60 °C and use shorter exposition times (~30 s). Moreover, it was observed that by modifying the input power and the treatment time, the area of the heated tissue that achieve ablation temperatures can be modified. This makes possible to treat different tumor sizes using the same antenna.

Table 2. Maximum temperatures reached by the antenna in the experiment and in the FEM model.

	Double Slot (5 cm of Antenna Insertion)					
	$T_{max\_30\ s}$ (°C)			$T_{max\_600\ s}$ (°C)		
	Slot 1	**Between the Slots**	**Slot 2**	**Slot 1**	**Between the Slots**	**Slot 2**
Meas	55.0	56.0	46.5	84.2	89.3	100.7
Sim	49.6	61.2	71.3	127.0	138.7	152.6

Figure 4 describes the comparison between the simulated and the measured temperature profiles generated by the double slot antenna (5 cm of antenna insertion). In the simulated temperature profiles, high temperatures, that keep increasing over the time, were obtained. The big temperature discrepancies between simulated and measured temperatures, star to be evident especially after 200 s, when the tissue reach temperatures around 90 °C. Therefore, these differences could be a consequence of the tissue denaturalization due to the reached temperature. Moreover, it is important to address that some dielectric and thermal tissue properties (e.g., dielectric permittivity) are temperature dependent; therefore, it is expected a change in the tissue properties during the treatment time. This effect is observed in the experimental evaluation. However, in the FEM modeling the temperature dependence was not considered, therefore the tissue temperature increased up to reach around 150 °C. To model the temperature dependence of tissue properties is still a challenge, especially at the ablation temperatures (60–100 °C). This is especially true because of the lack of tissue characterization at those temperatures.

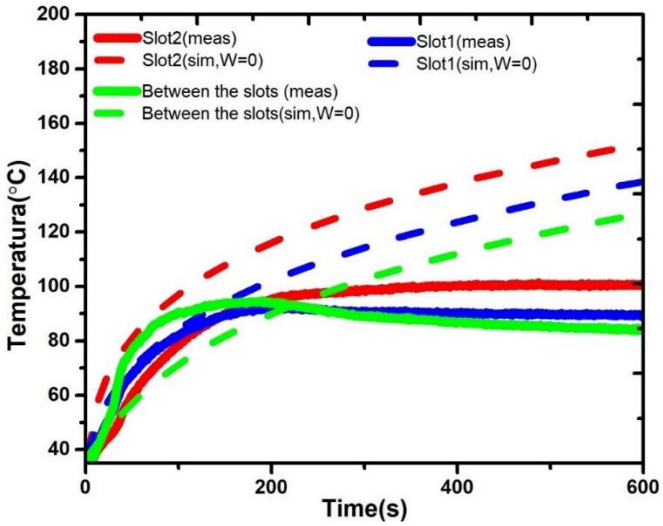

Figure 4. Temperature profiles obtained by the simulation (sim) versus temperature profiles obtained by the measurements from the experimentations (meas) for the double slot antenna with 5 cm of antenna insertion.

3.2. Thermal Ablation Experiments

3.2.1. Antenna Insertion

The SWR was measured by using the Agilent Technologies network analyzer (E5071B). This SWR measurement was carried out for each the experiments and the obtained values were around 1.5–1.8. Additionally, the ISYS245 microwave generator (Emblation Microwave, (Alloa, Scotland, UK)) provides the measurements of the reflected power; the obtained SWR values mean power losses lower than 1.5 W. The temperature increase generated by the antenna showed impact as a function of the antenna insertion. Figure 5a–c depict the temperature profiles generated by the double slot antenna at 3.5 and 5 cm of insertion. Three experiments were done for each antenna insertion. In all cases, the red line represents the temperature recorded from an antenna insertion of 3.5 cm, while the

blue line describes the temperature for an antenna insertion of 5 cm. Figure 5a,c depicts the temperatures recorded next to slot 1 and slot 2, respectively, while Figure 5b depicts the temperature increase recorded between the slots. In the upper side, a description of the location of the temperature sensors is depicted. Figure 5a–c show that the behavior of the double slot antenna is repeatable. However, if a comparison of 3.5 and 5 cm of antenna insertion is done, an impact over the temperature increase is observed (see Table 3). For 5 cm of antenna insertion, the temperature recorded by each sensor showed a uniform behavior over all the experiment. However, for an antenna insertion of 3.5 cm the sensors near to the surface of the bone and air (slot 2 and sensor between the slots) showed a decrease in temperature once both reached temperatures higher than 100 °C. This behavior can be a consequence of the nearness of the second slot to the surface of the bone and the surrounding air, leading to convection effects. During these experiments, after the tissue reached temperatures over 100 °C, the presence of bubbles was observed; then it is reasonable to attribute temperature decrease to convection effects. For 3.5 cm of antenna insertion, all the temperatures were into the ablation therapeutic range (60–100 °C), while for 5 cm, the temperature sensors recorded temperatures around 103 °C. Moreover, in all the cases, the temperature profiles generated for an antenna insertion of 5 cm were more uniform, i.e., no abrupt temperature changes were observed.

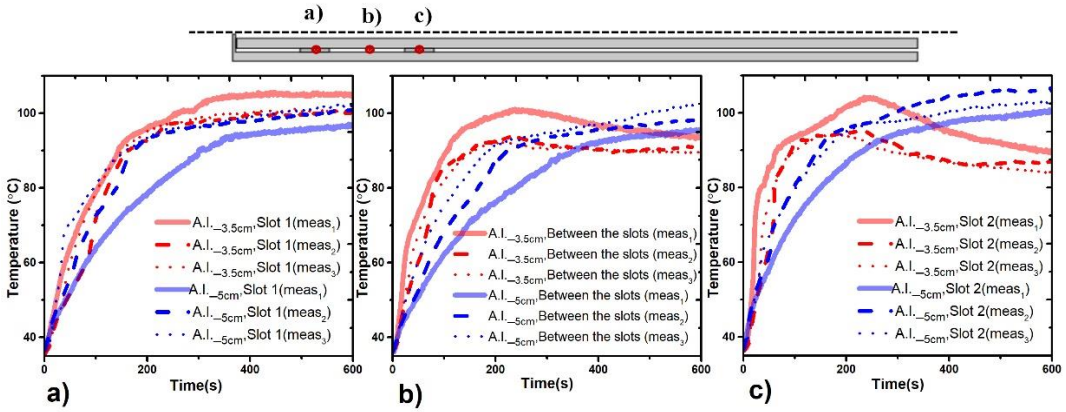

Figure 5. Temperature profiles generated by the double slot antenna located at different antenna insertions. (**a**) Temperature profiles recorded next to slot 1 of the antenna, (**b**) temperature profiles recorded at the middle point between the slots, (**c**) temperature profiles recorded next to slot 2 of the antenna. The red line represents the temperature recorded for an antenna insertion of 3.5 cm, while the blue line describes the temperature recorded for an antenna insertion of 5 cm.

Table 3. Maximum temperature elevations reached by the double slot antenna at different levels of antenna insertion.

	Antenna Insertion	
Sensor Location	**3.5 cm**	**5 cm**
Slot one	91.38 ± 2.17	99.67 ± 3.55
Slot two	102.07 ± 2.52	102.66 ± 2.77
Between the slots	87.05 ± 2.77	98.76 ± 3.21

3.2.2. Thermal Distributions

Figure 6 describes the thermal distribution generated by the double slot antenna, as well as the recorded temperature profiles. It is important to address that to be able to take a thermal image, the bone (porcine femur) was cut off by following the long middle axis line (see inset Figure 6b,d). After the experiment, the antenna was pulled out of the bone and the two pieces of bone were prepared for taking the thermal image. Figure 6a,b describe the behavior of the double slot antenna for an antenna insertion of 3.5 cm, while Figure 6c,d show the behavior for an antenna insertion of 5 cm. According to Figure 6b,d, in both

experiments, the heat distribution was uniformly spread around both slots. However, the temperature profiles describe some differences in the reached temperature. Temperature sensors located at the second slot recorded temperature increases of 55 °C and 43.92 °C for an antenna insertion of 3.5 cm and 5 cm, respectively. The sensor located at the first slot describes a different behavior in both cases: for 5 cm of antenna insertion; the sensor at the first slot follows a temperature increase (ΔT = 39.73 °C), similar to the one recorded by the sensor located at the second slot (ΔT = 43.92 °C). However, for 3.5 cm of antenna insertion, there was a difference between temperature increase at slot two (ΔT = 55 °C) and slot one (ΔT = 39.74 °C), of around 15 °C. These differences at the reached temperature are strongly related with the antenna insertion. On the other hand, the sensor located at 0.7 cm reached temperatures around 65 °C, enough temperature to ablate tissue. Finally, the sensors located at 1.4 cm reached temperatures higher than 50 °C, which means, once more, that either more time or higher input power are required to make the thermal ablation effective.

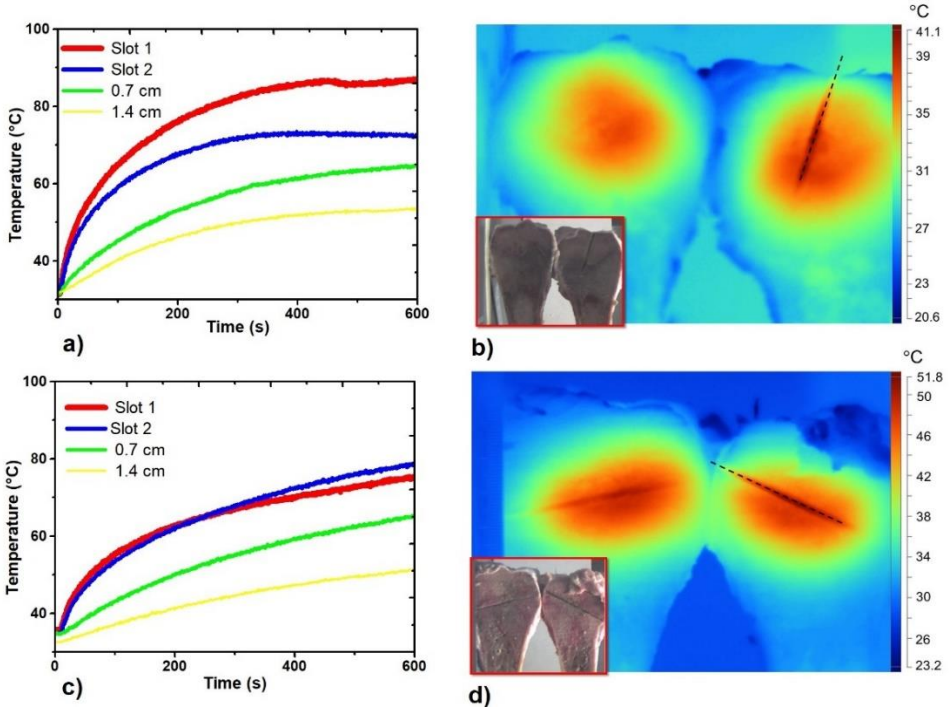

Figure 6. Temperature profiles and thermal distributions generated by the double slot antenna. (**a**) Temperature profiles generated by the antenna inserted at 3.5 cm; (**b**) Thermal distribution generated by the antenna inserted at 3.5 cm; (**c**) Temperature profiles generated by the antenna inserted at 5 cm; (**d**) Thermal distribution generated by the antenna inserted at 5 cm. The inset figure in (**b**,**d**) shows the two sections of the porcine bone, while the black dashed line describes the place where the antenna was inserted.

4. Discussion

The main goal of this paper was to design and evaluate the efficacy of a microwave antenna with two air slots to treat specifically bone tissue by thermal ablation. The experimental evaluation of the proposed antenna shows that their outcome makes it perfect to be used for thermal ablation in bone tissue, i.e., temperatures around 55 °C–100 °C were reached in the bone tissue, due to the EM field generated by the antenna. The experimental evaluation shows that the outcome generated by the antenna is repeatable. A big impact of the antenna insertion over the treatment outcome was found. Moreover, if the double slot antenna is inserted at 3.5 cm, temperatures recorded by the sensors closer to the surface tend to decrease once they reach temperatures above 100 °C. This is because of their nearness to the surface and the surrounding air. On the other hand, when the double slot antenna is inserted at 5 cm, the temperatures, recorded by the three sensors, follow the

same behavior through the experiment. The thermal distributions showed that the antenna can focus the EM energy near to the slots. The antenna showed a more uniform distribution around the heated area (see Figures 4 and 5), which means that a higher region can be treated by using this antenna. The antenna generated temperatures in the therapeutic range of thermal ablation. The focalization of the energy allows us to say that this antenna can be used to treat bone tumors without affecting the healthy surrounding tissue.

To our understanding, the proposed antenna is one of the a few specifically designed to treat hard tissue (bone tissue); therefore, a mayor efficiency is expected. The literature reports some studies, especially clinical applications where micro-coaxial antennas have been tested. However, these were commercial ones, i.e., they were designed to treat soft tissue. Pusceddu et al. report the treatment of bone metastases by using a delivered power of 50 W $\pm$ 20 per application times between 7 min $\pm$ 5 [17]. Meanwhile, Moser et al. report the use of 45 W for 10 min to treat bone tumors [55]. Moreover, Muheremu et al. report other clinical studies implemented to treat bone tumors where a delivered power around 80–120 W was applied per 20–30 min. In fact, up to 800 W applied per around 30–40 min have been also reported [56]. In our case, it was possible to generated thermal ablation in bone tissue by applying 10 W per 10 min. Moreover, it was observed that more input power can be applied to the antenna in order to reduce the treatment time and to modify the area of tissue affected by the temperature increase. However, to reduce the possibility to produce overheating in the surrounded healthy tissue, the use of less than 45 W as input power is expected. Although the proposed antenna shows a good performance, it could be improved, e.g., to regulate the antenna temperature, a cooling system must be designed. Moreover, the antenna can be redesigned by using a thicker gauge cable, to reduce the deformation due to its use. The necessity of the implementation of a system to locate the antenna and the temperature sensors in the correct places was observed, in order to record the temperature increase over the treated region, not only over a few points.

On the other hand, one of the main challenges in the modeling of thermal therapies is to get realistic thermal simulations. As previously mentioned, there is little information about the behavior of temperature dependence of tissue properties (especially in bone tissue) for higher temperatures, which makes it difficult to generate thermal models that appropriately describe the behavior of tissue during thermal ablation. Moreover, dielectric, and thermal properties for bone tumors have not been studied yet. Therefore, to develop theoretical and experimental studies, it is needed to evaluate the effect of different parameters (like perfusion, metabolism, etc.) over the model outcome. This study suggests that the use of thermo-dependent function to model dielectric and thermal properties of bone must be required. Moreover, special attention must be paid to temperatures higher than 80 °C and in the regions near to the air slots. It is important to remark that, to our understanding, until now, no study has been developed to compare theoretical and experimental evaluations for thermal ablation treatments in bone. The main goal of this comparison is to be able to generate thermal ablation treatment planning systems in the future.

5. Conclusions

This article shows the potential of a micro-coaxial double slot antenna to generate MW thermal ablation to treat bone tumors. The experimental results showed that the antenna is able to generate temperatures in the therapeutic range of the thermal ablation (60 °C–100 °C). The antenna generated thermal ablation in bone tissue by using the input power of 10 W applied for 10 min. The maximum measured SWR during the experimental evaluation was 1.8, which means a power loss lower than 1.5 W. This was due to the match between the antenna and the MW system. The antenna insertion modified the antenna behavior. For cases in which most of the antenna body is out of the bone, the reached temperatures were lower due to the nearness of the slot to the bone surface. An antenna insertion either equal or lower than 3.5 cm is not recommended because it modified the temperatures reached in the bone. However, one of the most important things is that the behavior of the antenna is repeatable. Finally, the temperature distributions showed a

heat concentration near to the antenna slots. The double slot antenna generates a thermal pattern distributed uniformly around both slots. This is a warranty that the surrounding healthy tissue is going to be less affected by the temperature increase.

Author Contributions: Conceptualization, C.J.T.-R.; Data curation, A.V.-H. and J.G.-M.; Formal analysis, C.J.T.-R. and L.L.-S.; Investigation, C.J.T.-R. and G.R.-M.; Methodology, C.J.T.-R. and G.R.-M.; Resources, L.L.-S., A.V.-H. and G.R.-M.; Software, L.L.-S., A.V.-H. and J.G.-M.; Supervision, L.L.-S., A.V.-H., G.R.-M. and J.G.-M.; Validation, A.V.-H. and G.R.-M.; Visualization, C.J.T.-R.; Writing—original draft, C.J.T.-R. All authors have read and agreed to the published version of the manuscript.

Funding: This research received no external funding.

Data Availability Statement: Data is contained within the article.

Acknowledgments: The authors thank to José Hugo Zepeda Peralta for his technical contribution to the development of the antenna and the experimental evaluation.

Conflicts of Interest: The authors declare no conflict of interest.

References

1. American Cancer Society Key Statistics for Bone Cancer. Available online: https://www.cancer.org/cancer/bone-cancer/about/key-statistics.html (accessed on 12 November 2020).
2. American Cancer Society Treating Bone Cancer. Available online: https://www.cancer.org/cancer/bone-cancer/treating.html (accessed on 22 March 2021).
3. Knavel, E.M.; Brace, C.L. Tumor Ablation: Common Modalities and General Practices. *Tech. Vasc. Interv. Radiol.* **2013**, *16*, 192–200. [CrossRef] [PubMed]
4. Stauffer, P.R. Evolving technology for thermal therapy of cancer. *Int. J. Hyperth.* **2005**, *21*, 731–744. [CrossRef] [PubMed]
5. Habash, R.W.Y.; Bansal, R.; Krewski, D.; Alhafid, H.T. Thermal Therapy, Part 1: An Introduction to Thermal Therapy. *Crit. Rev. Biomed. Eng.* **2006**, *34*, 459–489. [CrossRef] [PubMed]
6. Gebauer, B.; Tunn, P.-U. Thermal ablation in bone tumors. In *Minimally Invasive Tumor Therapies*; Springer: Berlin/Heidelberg, Germany, 2006; Volume 167, pp. 135–146.
7. Rhim, H.; Goldberg, S.N.; Dodd, G.D.; Solbiati, L.; Lim, H.K.; Tonolini, M.; Cho, O.K. Essential Techniques for Successful Radio-frequency Thermal Ablation of Malignant Hepatic Tumors. *RadioGraphics* **2001**, *21*, S17–S35. [CrossRef] [PubMed]
8. Riadh, W.Y.H.; Rajeev, B.; Daniel, K.; Hafid, T.A. Thermal therapy, Part III: Ablation techniques. *Crit. Rev. Biomed. Eng.* **2007**, *35*, 37–121.
9. Brace, C. Thermal Tumor Ablation in Clinical Use. *IEEE Pulse* **2011**, *2*, 28–38. [CrossRef]
10. Bertram, J.M.; Yang, D.; Converse, M.C.; Webster, J.G.; Mahvi, D.M. Antenna design for microwave hepatic ablation using an axisymmetric electromagnetic model. *Biomed. Eng. Online* **2006**, *5*, 15. [CrossRef]
11. Reeves, J.W.; Birch, M.J.; Hand, J.W. Comparison of simulated and experimental results from helical antennas within a muscle-equivalent phantom. *Phys. Med. Biol.* **2008**, *53*, 3057–3070. [CrossRef]
12. Ortega-Palacios, R.; Trujillo-Romero, C.J. Heat Transfer Study in Breast Tumor Phantom during Microwave Ablation: Modeling and Experimental Results for Three Different Antennas. *Electronics* **2020**, *9*, 535. [CrossRef]
13. Ortega-Palacios, R.; Trujillo-Romero, C.J.; Rubio, M.F.J.C.; Vera, A.; Leija, L.; Reyes, J.L.; Ramírez-Estudillo, M.C.; Morales-Alvarez, F.; Vega-Lopez, M.A. Feasibility of Using a Novel 2.45 GHz Double Short Distance Slot Coaxial Antenna for Minimally Invasive Cancer Breast Microwave Ablation Therapy: Computational Model, Phantom, and In Vivo Swine Experimentation. *J. Health Eng.* **2018**, *2018*, 1–10. [CrossRef]
14. López, G.D.G.; Rubio, M.F.J.C.; Jácquez, J.I.H.; Hernandez, A.V.; Salas, L.L.; Perezgasga, F.V.; García, F.F. Computational FEM Model, Phantom and Ex Vivo Swine Breast Validation of an Optimized Double-Slot Microcoaxial Antenna Designed for Minimally Invasive Breast Tumor Ablation: Theoretical and Experimental Comparison of Temperature, Size of Lesion, and SWR, Preliminary Data. *Comput. Math. Methods Med.* **2017**, *2017*, 1–11. [CrossRef]
15. Ito, K.; Yoshimura, H.; Hayashi, Y.; Saito, K. Heating characteristics of array applicator composed of two coaxial-slot antennas for microwave coagulation therapy. *IEEE Trans. Microw. Theory Tech.* **2000**, *48*, 1800–1806. [CrossRef]
16. Liu, F.-Y.; Yu, X.-L.; Liang, P.; Wang, Y.; Zhou, P.; Yu, J. Comparison of percutaneous 915 MHz microwave ablation and 2450 MHz microwave ablation in large hepatocellular carcinoma. *Int. J. Hyperth.* **2010**, *26*, 448–455. [CrossRef]
17. Pusceddu, C.; Sotgia, B.; Fele, R.M.; Melis, L. Treatment of Bone Metastases with Microwave Thermal Ablation. *J. Vasc. Interv. Radiol.* **2013**, *24*, 229–233. [CrossRef] [PubMed]
18. Gas, P. Multi–Frequency Analysis for Interstitial Microwave Hyperthermia Using Multi–Slot Coaxial Antenna. *J. Electr. Eng.* **2015**, *66*, 26–33. [CrossRef]
19. Piotr, G.A.S. Tissue Temperature Distributions for Different Frequencies derived from Interstitial Microwave Hyperthermia. *Prz. Elektrotech. arXiv* **2012**, arXiv:1710.00671.

20. Brace, C.L. Radiofrequency and Microwave Ablation of the Liver, Lung, Kidney, and Bone: What Are the Differences? *Curr. Probl. Diagn. Radiol.* **2009**, *38*, 135–143. [CrossRef]
21. Kurup, A.N.; Callstrom, M.R. Ablation of Musculoskeletal Metastases: Pain Palliation, Fracture Risk Reduction, and Oligometastatic Disease. *Tech. Vasc. Interv. Radiol.* **2013**, *16*, 253–261. [CrossRef] [PubMed]
22. Albisinni, U.; Bazzocchi, A.; Bettelli, G.; Facchini, G.; Castiello, E.; Cavaciocchi, M.; Battista, G.; Rotini, R. Treatment of osteoid osteoma of the elbow by radiofrequency thermal ablation. *J. Shoulder Elb. Surg.* **2014**, *23*, e1–e7. [CrossRef]
23. Fan, Q.-Y.; Ma, B.-A.; Zhou, Y.; Zhang, M.-H.; Hao, X.-B. Bone Tumors of the Extremities or Pelvis Treated by Micro-wave-Induced Hyperthermia. *Clin. Orthop. Relat. Res.* **2003**, *406*, 165–175. [CrossRef]
24. Filippiadis, D.K.; Tutton, S.; Kelekis, A. Percutaneous bone lesion ablation. *Radiol. Med.* **2014**, *119*, 462–469. [CrossRef] [PubMed]
25. Ringe, K.I.; Panzica, M.; Von Falck, C. Thermoablation of Bone Tumors. *Fortschr. Röntgenstr.* **2016**, *188*, 539–550. [CrossRef]
26. Debnath, O.B.; Saito, K.; Ito, K.; Uesaka, M. Breast cancer treatment by combining microwave hyperthermia and radiation brachytherapy. In Proceedings of the 2016 International Symposium on Antennas and Propagation (ISAP), Okinawa, Japan, 24–28 October 2016; pp. 472–473.
27. Leggio, L.; de Varona, O.; Dadrasnia, E. A comparison between different schemes of microwave cancer hyperthermia treatment by means of left-handed metamaterial lenses. *Prog. Electromagn. Res.* **2015**, *150*, 73–87. [CrossRef]
28. Dupuy, D.E.; Goldberg, S.N. Image-guided Radiofrequency Tumor Ablation: Challenges and Opportunities—Part II. *J. Vasc. Interv. Radiol.* **2001**, *12*, 1135–1148. [CrossRef]
29. Carrafiello, G.; Laganà, D.; Mangini, M.; Fontana, F.; Dionigi, G.; Boni, L.; Rovera, F.; Cuffari, S.; Fugazzola, C. Microwave tumors ablation: Principles, clinical applications and review of preliminary experiences. *Int. J. Surg.* **2008**, *6*, S65–S69. [CrossRef]
30. Trujillo-Romero, C.; Rico-Martinez, G.; Leija-Salas, L.; Vera-Hernandez, A.; Gutierrez-Martinez, J. Microwave ablation to treat bone tumors by using a double slot antenna: A modelling study. *Pan Am. Health Care Exch. PAHCE* **2017**, 66–69. [CrossRef]
31. Lujan, F.; Pinilla, B.; Gutierrez-Martinez, J.; Vera-Hernandez, A.; Leija, L.; Trujillo-Romero, C.J. Theoretical model of MW antennas to treat bone tumors: One slot and one slot choked antennas. In Proceedings of the 2017 14th International Conference on Electrical Engineering, Computing Science and Automatic Control (CCE), Mexico City, Mexico, 20–22 October 2017; pp. 1–6.
32. Ramirez-Guzman, T.; Trujillo-Romero, C.; Vera-Hernandez, A.; Leija, L. Micro-coaxial monopole antenna to treat bone cancer: Design and preliminary experimentation. In Proceedings of the 2019 Global Medical Engineering Physics Exchanges/Pan American Health Care Exchanges (GME-PE/PAHCE), Buenos Aires, Argentina, 26–31 March 2019; pp. 1–6.
33. Martinez-Valdez, R.; Trujillo-Romero, C.; Castellanos, L.; Gutierrez-Martinez, J.; Vera-Hernandez, A.; Ramos, A.; Leija, L. Feasibility of the microwave and ultrasound ablation as alternatives to treat bone tumors. *Pan Am. Health Care Exch. PAHCE* **2017**, 1–6. [CrossRef]
34. Trujillo, C.J.; Rico, G.; Leija, L.; Vera, A.; Gutiérrez, J.; Ieee, M. Micro-Coaxial Slot Antenna to Treat Bone Tumors by Thermal Ablation: Theoretical and Experimental Evaluation. *IEEE Lat. Am. Trans.* **2018**, *16*, 2731–2737. [CrossRef]
35. Karampatzakis, A.; Kühn, S.; Tsanidis, G.; Neufeld, E.; Samaras, T.; Kuster, N. Heating characteristics of antenna arrays used in microwave ablation: A theoretical parametric study. *Comput. Biol. Med.* **2013**, *43*, 1321–1327. [CrossRef] [PubMed]
36. Alnassan, H.; Kastler, A.; Wang, X.; Kastler, B. Targeted radiation dipole antenna using 3D numerical simulation in microwave ablation. In Proceedings of the International Conference on Biomedical Electronics and Devices, Lisbon, Portugal, 12–15 January 2015.
37. Capek, L.; Henys, P.; Barsa, P.; Dvorak, V. Performance of radiofrequency ablation used for metastatic spinal tumor: Numerical approach. *Proc. Inst. Mech. Eng. Part H J. Eng. Med.* **2017**, *231*, 814–820. [CrossRef]
38. Denzi, A.; Strigari, L.; Di Filippo, F.; Botti, C.; Di Filippo, S.; Perracchio, L.; Ronchetti, M.; Cadossi, R.; Liberti, M. Modeling the positioning of single needle electrodes for the treatment of breast cancer in a clinical case. *Biomed. Eng. Online* **2015**, *14*, S1. [CrossRef] [PubMed]
39. Fang, Z.; Zhang, B.; Moser, M.; Zhang, E.; Zhang, W. Design of a Novel Electrode of Radiofrequency Ablation for Large Tumors: A Finite Element Study. *J. Eng. Sci. Med. Diagn. Ther.* **2017**, *1*, 011001. [CrossRef]
40. Scott, S.J.; Prakash, P.; Salgaonkar, V.; Jones, P.D.; Cam, R.N.; Han, M.; Rieke, V.; Burdette, E.C.; Diederich, C.J. Approaches for modelling interstitial ultrasound ablation of tumours within or adjacent to bone: Theoretical and experimental evaluations. *Int. J. Hyperth.* **2013**, *29*, 629–642. [CrossRef] [PubMed]
41. Tian, Z.; Dong, T.; Cheng, Y.; Hu, J.; Nan, Q. A Treatment Planning of Radio Frequency Ablation for Spinal Tumor. *Int. J. Comput. Methods* **2019**, *16*, 1842005. [CrossRef]
42. Keangin, P.; Rattanadecho, P.; Wessapan, T. An analysis of heat transfer in liver tissue during microwave ablation using single and double slot antenna. *Int. Commun. Heat Mass Transf.* **2011**, *38*, 757–766. [CrossRef]
43. Hasgall, P.; Neufeld, E.; Gosselin, M.; Klingenbock, A.; Kuster, N. IT'IS Database for Thermal and Electromagnetic Parameters of Biological Tissues. Available online: http://www.itis.ethz.ch/itis-for-health/tissue-properties/overview/ (accessed on 22 March 2021).
44. Brace, C.L. Dual-slot antennas for microwave tissue heating: Parametric design analysis and experimental validation. *Med. Phys.* **2011**, *38*, 4232–4240. [CrossRef] [PubMed]
45. Jin, J.-M.; Lou, Z.; Li, Y.-J.; Riley, N.W.; Riley, D.J. Finite Element Analysis of Complex Antennas and Arrays. *IEEE Trans. Antennas Propag.* **2008**, *56*, 2222–2240. [CrossRef]
46. Sysoev, S.; Kislitsy, A. Modeling of Microwave Heating and Oil Filtration in Stratum. *Numer. Simul. Appl. Ex. Theory* **2011**. [CrossRef]

47. Ibitoye, A.Z.; Adeneye, S.O.; Akpochafor, M.O.; Nwoye, E.O.; Aweda, M.A. Finite Element Analysis of Single Slot Antenna for Microwave Tumor Ablation. *IOSR J. Appl. Phys.* **2014**, *5*, 55–62. [CrossRef]
48. Gas, P. SAR optimization for multi-dipole antenna array with regard to local hyperthermia. *Prz. Elektrotech.* **2019**, *1*, 19–22. [CrossRef]
49. Gas, P. Optimization of multi-slot coaxial antennas for microwave thermotherapy based on the S 11 parameter analysis. *Biocybern. Biomed. Eng.* **2017**, *37*, 78–93. [CrossRef]
50. Gabriel, S.; Lau, R.W.; Gabriel, C. The dielectric properties of biological tissues: II. Measurements in the frequency range 10 Hz to 20 GHz. *Phys. Med. Biol.* **1996**, *41*, 2251–2269. [CrossRef]
51. Pennes, H.H. Analysis of Tissue and Arterial Blood Temperatures in the Resting Human Forearm. *J. Appl. Physiol.* **1998**, *85*, 5–34. [CrossRef] [PubMed]
52. Ernesto, J.; Aguayo, L. *Proposed Treatment for Breast Cancer Ablation with Core-Shell Nanoparticles Excited by 2.45 GHz Specifically Optimized Microcoaxial Antennas*; Center for Research and Advanced Studies of the National Polytechnic Institute (CINVESTAV): Mexico City, Mexico, 2016.
53. Huang, Y.; Boyle, K. *Antennas: From Theory to Practice*; Wiley: Hoboken, NJ, USA, 2008; ISBN 9780470510285.
54. Gabriel, C.; Gabriel, S.; Corthout, E. The dielectric properties of biological tissues: I. Literature survey. *Phys. Med. Biol.* **1996**, *41*, 2231–2249. [CrossRef]
55. Moser, T.; Buy, X.; Goyault, G.; Tok, C.; Irani, F.; Gangi, A. Ablation des tumeurs osseuses sous contrôle de l'imagerie: Revue des techniques actuelles. *J. Radiol.* **2008**, *89*, 461–471. [CrossRef]
56. Niu, X.; Muheremu, A. Microwave Ablation for Bone Tumors. *Orthop. Muscular Syst.* **2014**, *3*, 1–4. [CrossRef]